ELSEVIER

Physica B 273–274 (1999) 33–38

PHYSICA B

www.elsevier.com/locate/physb

Observation of Ga vacancies and negative ions in undoped and Mg-doped GaN bulk crystals

K. Saarinen[a,*], J. Nissilä[a], J. Oila[a], V. Ranki[a], M. Hakala[a], M.J. Puska[a], P. Hautojärvi[a], J. Likonen[b], T. Suski[c], I. Grzegory[c], B. Lucznik[c], S. Porowski[c]

[a]*Laboratory of Physics, Helsinki University of Technology, P.O. Box 1100, 02015 HUT, Finland*
[b]*Technical Research Centre of Finland, Chemical Technology, P.O. Box 1404, 02044 VTT, Finland*
[c]*UNIPRESS, High Pressure Research Center, Polish Academy of Sciences, 01-142 Warsaw, Poland*

Abstract

Gallium vacancies and negative ions are observed in GaN bulk crystals by applying positron lifetime spectroscopy. The concentration of Ga vacancies decreases with increasing Mg doping, as expected from the behavior of the V_{Ga} formation energy as a function of the Fermi level. The concentration of negative ions correlates with that of Mg impurities determined by secondary ion mass spectrometry. We thus attribute the negative ions to Mg_{Ga}^{-}. The negative charge of Mg suggests that Mg doping converts n-type GaN to semi-insulating mainly due to the electrical compensation of O_N^+ donors by Mg_{Ga}^{-} acceptors.

Keywords: GaN; Vacancies; Compensation; Positrons

1. Introduction

Bulk GaN crystals are ideal substrates for the epitaxy of GaN overlayers for optoelectronic components at the blue wavelength. Such material can be synthesized of liquid Ga in high N overpressure at elevated temperatures [1]. Nominally undoped GaN crystals show usually high n-type conductivity with the concentration of electrons exceeding 10^{19} cm^{-3}. This is most likely due to the residual oxygen atoms acting as shallow donors [2,3]. When GaN is doped with Mg the electron concentration decreases and for sufficiently high amount of Mg dopants the samples become semi-insulating. It is interesting to study how the movement of the Fermi level toward the midgap changes the formation of charged native defects such as the Ga vacancy. Another basic question concerns the mechanism of the electrical deactivation. One can consider either (i) the gettering role of Mg leading to the formation of MgO molecules [4] or (ii) electrical compensation of O_N^+ donors by Mg_{Ga}^{-} acceptors.

Positrons in solids get trapped at neutral and negative vacancy defects, which can be experimentally detected by measuring the positron lifetime [5]. At low temperatures positrons are also captured at the hydrogenic states around negative ions. The positron experiments thus yield detailed information on the concentration and structure of intrinsic and extrinsic acceptors. Our previous results have indicated that negative Ga vacancies are formed during the growth of undoped n-type GaN crystals and epitaxial layers [6,7]. There is also evidence that the creation of V_{Ga} is less likely in semi-insulating or p-type GaN overlayers on sapphire [7,8].

In this paper we review our recent works [6,9] and show that Ga vacancy acts as a native defect in GaN crystals. We pay special attention to the identification of V_{Ga} by correlating the results of positron experiments with those of theoretical calculations. Our data indicate that the formation of Ga vacancies is suppressed by Mg doping. We show further that most of Mg is in a negative charge state, suggesting that the loss of n-type conductivity is due to compensation of O_N^+ donors by Mg_{Ga}^{-} acceptors.

* Corresponding author. Tel.: + 358-9-451-3111; fax: + 358-9-451-3116.
E-mail address: ksa@fyslab.hut.fi (K. Saarinen)

0921-4526/99/$ - see front matter
PII: S0921-4526(99)00400-7

2. Experimental details and data analysis

The bulk GaN crystals were grown at the nitrogen pressure of 1.5 GPa and temperature of 1500°C [1]. We studied three samples, where the Mg doping level was intentionally varied during the crystal growth (Table 1). The Mg and O concentrations of the samples were determined experimentally by secondary ion-mass spectrometry (SIMS). The absolute concentrations were calibrated by implanting known amounts of O and Mg to undoped epitaxial GaN layers, where the residual Mg and O concentrations were well below 10^{18} cm^{-3}.

The positron lifetime experiments were performed using conventional instrumentation by sandwiching two identical sample pieces with a 30 μCi ^{22}Na positron source [5]. The lifetime spectrum is a sum of exponential decay components $-\mathrm{d}n(t)/\mathrm{d}t = \sum_i (I_i/\tau_i)\exp(-t/\tau_i)$, where $n(t)$ is the probability of positron to be alive at time t. The positron in the state i (e.g. delocalized state in the lattice or localized state at a vacancy) annihilates with the lifetime τ_i and the intensity I_i. The increase of the average lifetime $\tau_{av} = \sum I_i \tau_i$ above τ_B obtained in the defect-free lattice is a clear sign of vacancy defects in the sample.

The Doppler broadening of the 511 keV annihilation radiation was recorded using a Ge detector with an energy resolution of 1.4 keV. These measurements yield the one-dimensional momentum distribution of electrons as seen by the positron. In order to observe annihilations with core electrons, the experimental background was reduced by detecting simultaneously the two annihilation photons [10]. For this purpose, a NaI detector was placed collinearly with the Ge detector and a coincidence between the two detectors was electronically required.

In order to help the interpretation of the experimental results we calculated the positron lifetime and core electron momentum density theoretically [10,11]. The electron densities were constructed using the atomic superposition method. The positron states were solved in a supercell of 256 atomic sites in a periodic superlattice using the generalized gradient approximation for electron–positron correlation. The core electron momentum distribution seen by the positron was calculated using atomic wave functions for core electrons and the state-dependent enhancement scheme [11].

3. Impurity concentrations

The secondary ion-mass spectrometry indicates that the oxygen concentration is about 4×10^{19} cm^{-3} in undoped GaN (Table 1). The concentration of conduction electrons ($n = 5 \times 10^{19}$ cm^{-3} at 300 K) in this sample is thus almost the same as oxygen concentration. This is in good agreement with the previous evidence [2,3] that the n-type conductivity of GaN is due to unintentional oxygen doping. In the lightly Mg doped GaN the concentration of oxygen is 12×10^{19} cm^{-3}, which is slightly larger than the Mg concentration of 6×10^{19} cm^{-3}. The electrical experiments indicate that the sample has n-type conductivity, but the carrier concentration is less than in the undoped sample. The heavily Mg-doped sample has the O concentration of 9×10^{19} cm^{-3} and the Mg concentration of 1×10^{20} cm^{-3}. According to the electrical experiments the sample is semi-insulating. This is reasonable since the impurity concentrations determined by SIMS show that [Mg] ≈ [O].

4. Positron lifetime results

Examples of positron lifetime spectra are shown in Fig. 1 and the temperature dependencies of the average lifetime τ_{av} and the second lifetime component τ_2 are presented in Fig. 2. In the lifetime experiment of Fig. 1, positrons enter the sample and thermalize at the time $t = 0$. The vertical axis gives the number of annihilations at a time interval of 25 ps. In the heavily Mg-doped sample the positron lifetime spectrum has a single component of 165 ± 1 ps at 300 K. The lifetime is almost constant as a function of temperature (Fig. 2).

Both these observations indicate that the heavily Mg-doped GaN is free of vacancy defects trapping positrons. In perfect GaN lattice the positron state is very delocalized and the positron density has its maximum in the interstitial region (Fig. 3). The calculated lifetime in defect-free GaN lattice is 154 ps, which is in reasonable agreement with the experimental result $\tau_B = 165$ ps. The lifetime $\tau_B = 165$ ps is also very close to our earlier estimate (166 ps) based on the lifetime decomposition at low temperature [6]. In heavily Mg-doped GaN all positrons

Table 1
The concentrations of impurities and defects in the studied GaN bulk crystals. The magnesium and oxygen concentrations were determined by secondary ion mass spectrometry. The concentrations of Ga vacancies and negative ions are obtained from the positron annihilation data [9]

Sample	Oxygen concentration (cm^{-3})	Magnesium concentration (cm^{-3})	Ga vacancy concentration (cm^{-3})	Negative ion concentration (cm^{-3})
Undoped	4×10^{19}	1×10^{18}	2×10^{17}	3×10^{18}
Lightly Mg doped	12×10^{19}	6×10^{19}	7×10^{16}	6×10^{19}
Heavily Mg doped	9×10^{19}	10×10^{19}	$< 10^{16}$	

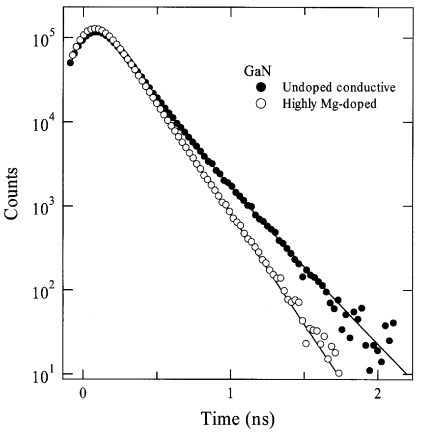

Fig. 1. Examples of positron lifetime spectra in undoped and highly Mg-doped GaN bulk crystals. The data are normalized to the typical experimental integral of 2×10^6 counts. The solid lines are fits to the sum of exponential decay components convoluted with the resolution function of the spectrometer. The data in the highly Mg-doped sample (recorded at 300 K) has only a single component of 165 ± 1 ps. The spectrum in the undoped crystal (recorded at 490 K) can be decomposed into two components of $\tau_1 = 150 \pm 10$ ps, $\tau_2 = 235 \pm 5$ ps, and $I_2 = 48 \pm 6\%$ [9].

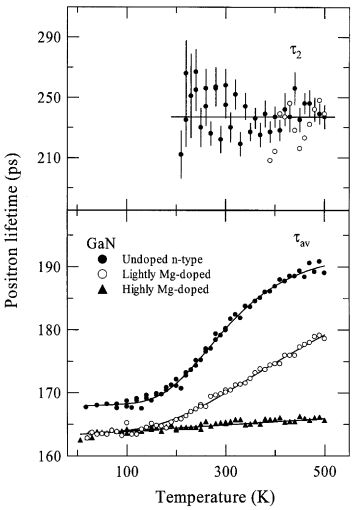

Fig. 2. The average positron lifetime and the second lifetime component τ_2 versus measurement temperature in GaN bulk crystals. The solid lines correspond to the analyses with the temperature-dependent positron trapping model, where concentrations of Ga vacancies and negative ions (Table 1) are determined as fitting parameters.

thus annihilate in the delocalized state in the GaN lattice with the bulk lifetime $\tau_B = 165$ ps. The slight increase of the bulk lifetime as a function of temperature (Fig. 2) can be attributed to the lattice expansion.

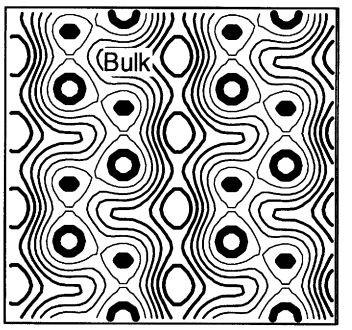

Fig. 3. The delocalized positron density in perfect GaN lattice according to theoretical calculations. The c-axis of the wurtzite structure is vertical in the figure. The positions of the Ga and N atoms are marked with open circles and diamonds, respectively. The contour spacing is $\frac{1}{6}$ of the maximum value.

The positron lifetime spectrum recorded in undoped GaN is clearly different from that in highly Mg-doped sample (Fig. 1). The annihilation probability at $t > 0.5$ ns is much larger in the undoped GaN, indicating that the average positron lifetime τ_{av} is longer than $\tau_B = 165$ ps. In fact, $\tau_{av} = 167$ ps at $T = 10$–150 K, and it increases up to $\tau_{av} = 190$ ps at 500 K (Fig. 2). In lightly Mg-doped GaN the positron lifetime is equal to $\tau_B = 165$ ps at low temperatures of 10–200 K (Fig. 2). At 200–500 K, however, τ_{av} is clearly larger than τ_B and reaches a value of 180 ps at 500 K. Since $\tau_{av} > \tau_B$ in both undoped and lightly Mg-doped samples, we can conclude that these GaN crystals contain vacancy defects.

The lifetime spectra recorded at 300–500 K in the undoped and lightly Mg-doped GaN can be decomposed into two exponential components (Figs. 1 and 2). The positrons trapped at vacancies annihilate with the longer lifetime $\tau_V = \tau_2 = 235 \pm 5$ ps. Within experimental accuracy this lifetime is the same in the n-type undoped crystal and in the lightly Mg-doped sample (Fig. 2), indicating that the same vacancy is present.

5. Doppler broadening results

The high-momentum part of the Doppler broadening spectrum was recorded in n-type GaN overlayers, which contain the same vacancy defect as the bulk crystals [6]. This experiment yields the superimposed electron momentum distribution $\rho(p) = (1 - \eta_V)\rho_B(p) + \eta_V \rho_V(p)$, where $\rho_B(p)$ and $\rho_V(p)$ are the momentum distributions in the lattice and at the vacancy, respectively. η_V is the fraction of positrons annihilating at the vacancy, which can be determined using the positron trapping model and the combination of positron lifetime and Doppler experiments [6]. Since the momentum distribution in the lattice $\rho_B(p)$ can be measured in the defect-free reference sample

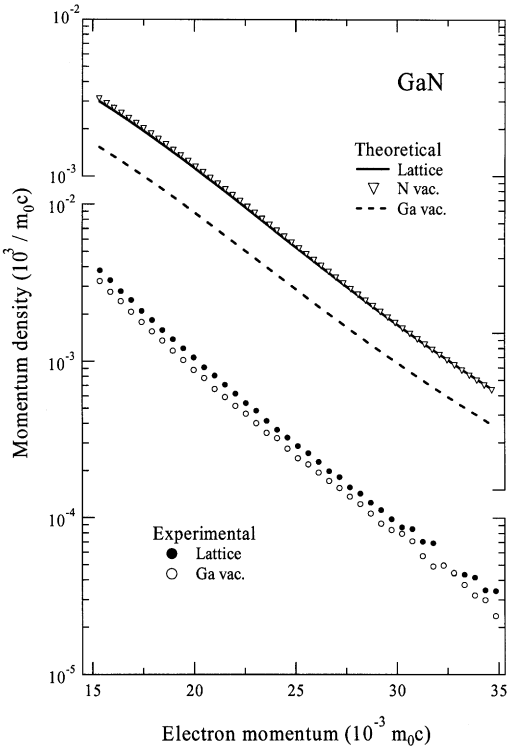

Fig. 4. The lower panel presents experimental core electron momentum densities at the perfect GaN lattice and at the Ga vacancy. The upper panel shows the result of the theoretical calculation at perfect GaN and at N and Ga vacancies. The momentum distibutions are normalized to unity.

such as heavily Mg-doped GaN crystal, the distributions $\rho_V(p)$ at vacancies can be decomposed from the measured spectrum $\rho(p)$.

Fig. 4 shows the core electron momentum distributions $\rho_B(p)$ and $\rho_V(p)$ in the perfect GaN lattice and at the vacancy defect, respectively. The intensity of the core electron momentum distribution is clearly smaller in the vacancy than in the GaN lattice. However, the momentum distributions at vacancies and in the bulk have clearly similar shapes over a wide momentum range.

6. Identification of the vacancy defect

Positron trapping and annihilation with the lifetime $\tau_V = 235$ ps is observed at native vacancies in n-type GaN crystals. This value is typical for a monovacancy in materials which have the same atomic density as GaN, such as Al. The calculated positron densities at Ga and N vacancies are shown in Figs. 5 and 6. Both vacancies are able to localize the positron. However, the localization is clearly stronger in the case of Ga vacancy, because the open volume of V_{Ga} is much larger than that of V_N.

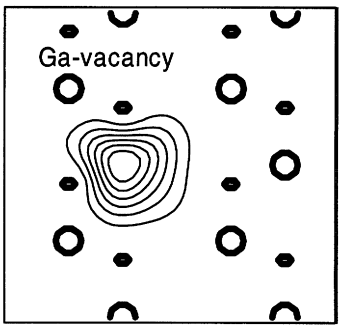

Fig. 5. The localized positron density in an ideal Ga vacancy in GaN according to theoretical calculations. The c-axis of the wurtzite structure is vertical in the figure. The positions of the Ga and N atoms are marked with open circles and diamonds, respectively. The contour spacing is $\frac{1}{6}$ of the maximum value.

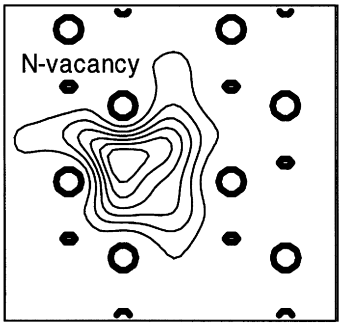

Fig. 6. The localized positron density in an ideal N vacancy in GaN according to theoretical calculations. The c-axis of the wurtzite structure is vertical in the figure. The positions of the Ga and N atoms are marked with open circles and diamonds, respectively. The contour spacing is $\frac{1}{6}$ of the maximum value.

This fact is reflected in the calculated positron lifetimes, which are $\tau_V = 209$ and 160 ps for unrelaxed Ga and N vacancies, respectively. The experimental value of 235 ps can thus be associated with the Ga vacancy but not with the N vacancy.

The same identification can be deduced on the basis of the Doppler broadening experiments. The calculations show that the annihilations with Ga 3d electrons give the clearly dominant contribution to the measured core electron momentum distribution at GaN lattice as well as at Ga and N vacancies. The shape of the momentum distributions is thus similar in all these three systems. The calculated momentum distribution at the Ga vacancy clearly has a lower intensity than that in the GaN lattice (Fig. 4), because the contribution of Ga 3d is reduced due to the surrounding N atoms. At the N vacancy the neighboring Ga atoms yield a core annihilation component, which is as strong as in the bulk lattice

(Fig. 4). The experimental curve is compatible with the Ga vacancy, but not with the N vacancy.

The combination of positron lifetime and Doppler broadening experiments thus unambiguously shows that the native vacancies in GaN crystals belong to the Ga sublattice and have an open volume of a monovacancy. According to theoretical calculations [12,13], the Ga vacancy is negatively charged in n-type and semi-insulating GaN and thus acts as an efficient positron trap. On the other hand, the N vacancy is expected to be positive and repulsive to positrons [12,13]. The calculated difference $\tau_V - \tau_B$ becomes equal to the experimental value $\tau_V - \tau_B = 70$ ps when the neighboring N atoms are relaxed 5% outwards from the Ga vacancy. In fact, an outwards relaxation is expected for the Ga vacancy on the basis of theoretical calculations [12,13]. Unfortunately, the present positron experiments do not tell whether V_{Ga} is an isolated defect or part of a larger complex.

7. Positron trapping at negative ions

The decrease of the average lifetime at low temperatures (Fig. 2) indicates that the fraction $\eta_V = (\tau_{av} - \tau_B)/(\tau_V - \tau_B)$ of positrons annihilating at vacancies decreases. Since the positron trapping at negative Ga vacancies should be enhanced at low temperatures [14], the decrease of η_V is due to other defects which compete with Ga vacancies as positron traps. Negative ions are able to bind positrons at shallow (< 0.1 eV) hydrogenic states in their attractive Coulomb field [5]. Since they possess no open volume, the lifetime of positrons trapped at them is the same as in the defect-free lattice, $\tau_{ion} = \tau_B = 164 \pm 1$ ps. The average lifetime increases above 150 K when positrons start to escape from the ions and a larger fraction of them annihilates at vacancies.

The temperature dependence of the average lifetime can be modeled with kinetic trapping equations [5]. Positron trapping coefficients at negative Ga vacancies μ_V and negative ions μ_{ion} vary as $T^{-1/2}$, a function of temperature [5,14]. The positron detrapping rate from the ions can be expressed as $\delta(T) \propto \mu_{ion} T^{-3/2} \exp(-E_{ion}/k_B T)$, where E_{ion} is the positron binding energy at the Rydberg state of the ions. The fraction of annihilations η_V at Ga vacancies depends on the concentrations c_V and c_{ion} of Ga vacancies and negative ions, respectively, as well as on the detrapping rate $\delta(T)$. We take the conventional value $\mu_V = 2 \times 10^{15}\ s^{-1}$ for the positron trapping coefficient at 300 K [5]. The average lifetime $\tau_{av} = (1 - \eta_V)\tau_B + \eta_V \tau_V$ can be fitted to the experimental data of Fig. 2 with c_V, c_{ion}, μ_{ion} and E_{ion} as adjustable parameters. As indicated by the solid lines in Fig. 2, the fits reproduce well the experimental data with the positron binding energy of $E_{ion} = 60 \pm 10$ meV and trapping coefficient $\mu_{ion} = (7 \pm 4) \times 10^{16} (T/K)^{-0.5}$. These values are close to those obtained previously in GaAs [5].

8. Defect concentrations and electrical deactivation

The analysis explained above yields estimates for the concentrations of V_{Ga} and negative ions (Table 1). The Ga vacancy concentration is $c_V = 2 \times 10^{17}\ cm^{-3}$ in the undoped GaN and $c_V = 7 \times 10^{16}\ cm^{-3}$ in the lightly Mg-doped crystal. In the heavily Mg-doped GaN no Ga vacancies are observed indicating that their concentration is below the detection limit of $10^{16}\ cm^{-3}$. The concentration of V_{Ga} thus decreases with increasing Mg doping and the Ga vacancies disappear completely when the material gets semi-insulating, i.e. [O] $\approx$ [Mg]. The same observation has been done also in Mg-doped GaN layers on sapphire [8,15]. This behavior is in good agreement with the results of theoretical calculations, which predict a low energy formation for the Ga vacancy and V_{Ga}–O_N complex only in n-type material [12,13]. The creation of Ga vacancies in the growth of GaN crystals seems to follow thus the trends expected for acceptor defects in thermal equilibrium.

The concentration of negative ions is $3 \times 10^{18}\ cm^{-3}$ in undoped GaN and about $6 \times 10^{19}\ cm^{-3}$ in lightly Mg-doped crystal. The ion concentration cannot be determined in heavily Mg-doped sample because no competitive positron trapping at Ga vacancies is observed and the positron annihilations at the ions cannot be distinguished from those in the GaN lattice. Due to the uncertainties in the values of positron trapping coefficients μ_V and μ_{ion} the experimental errors of the absolute concentrations of negative ions are large, of the order of 50%. In the lightly Mg doped sample c_{ion} represents the lower limit concentration only, because at temperatures of $T < 200$ K the average lifetime saturates at the value τ_B corresponding to annihilations in the GaN lattice.

In spite of the experimental inaccuracies the data indicates clearly that the concentration of negative ions increases by at least an order of magnitude with the Mg doping. Furthermore, the estimated concentrations of negative ions are close to those of Mg impurities as determined by the SIMS measurements (Table 1). Hence, it is natural to attribute the negative ions to Mg_{Ga}^{-}. The positron results thus show that a substantial part of the Mg impurities is in the negative charge state in Mg-doped GaN bulk crystals. This suggests that the conversion of n-type GaN to semi-insulating with Mg doping is mainly due to an electrical compensation of oxygen donors with negatively charged Mg acceptors. The electrons originating from O donors are transferred to Mg acceptors charging them negatively. Since positron trapping at Mg_{Ga}^{-} requires long-range Coulomb attraction,

we can infer that Mg_{Ga}^{-} ions are not spatially correlated with positive O_N^+ donors. However, we cannot exclude the formation of MgO molecules [4], which may also contribute to some extent to the electrical deactivation of Mg-doped GaN crystals.

9. Conclusions

The positron experiments show the presence of Ga vacancies and negative ions in GaN crystals. The concentration of Ga vacancies decreases with increasing Mg doping, in good agreement with the trends expected for the V_{Ga} formation energy as a function of the Fermi level. The concentration of negative ions increases with Mg doping and correlates with the Mg concentration determined by SIMS. We thus associate the negative ions with Mg_{Ga}^{-}. The negative charge of Mg suggests that the loss of n-type conductivity in the Mg doping of GaN crystals is mainly due to compensation of O_N^+ donors by Mg_{Ga}^{-} acceptors.

Acknowledgements

The authors would like to acknowledge the financial support from the Academy of Finland (EPI-2 project) and the State Committee for Scientific Research (Poland) (Grant KBN 7T08A 007 13).

References

[1] S. Porowski et al., in: S.J. Pearton (Ed.), GaN and Related Materials, Vol. 2, Gordon and Breach, Amsterdam, 1997, p. 295.
[2] C. Wetzel et al., Phys. Rev. Lett. 78 (1997) 3923.
[3] T. Suski et al., in: J.I. Pankove, T.D. Moustakas (Eds.), Gallium Nitride (GaN) I, Vol. 50, Academic Press, San Diego, 1998, p. 279.
[4] J.I. Pankove et al., Appl. Phys. Lett. 74 (1999) 416.
[5] K. Saarinen et al., in: M. Stavola (Ed.), Identification of Defects in Semiconductors, Academic Press, New York, 1998, p. 209.
[6] K. Saarinen et al., Phys. Rev. Lett. 79 (1997) 3030.
[7] K. Saarinen et al., Appl. Phys. Lett. 73 (1998) 3253.
[8] L.V. Jorgensen et al., Mater Res. Soc. Symp. Proc. 449 (1997) 853.
[9] K. Saarinen et al., Appl. Phys. Lett. 75 (1999) 2441.
[10] M. Alatalo et al., Phys. Rev. B 51 (1995) 4176.
[11] M. Alatalo et al., Phys. Rev. B 54 (1996) 2397.
[12] J. Neugebauer et al., Appl. Phys. Lett. 69 (1996) 503.
[13] T. Mattila et al., Phys. Rev. B 55 (1997) 9571.
[14] M.J. Puska et al., Rev. Mod. Phys. 66 (1994) 841.
[15] J. Oila et al., 1999, unpublished.